JOURNAL OF MATERIALS SCIENCE 30 (1995) 2412–2419

A d.c. plasma-fluidized bed reactor for the production of calcium carbide

C. W. ZHU, G. Y. ZHAO*, V. HLAVACEK
Ceramic and Reaction Engineering Laboratory, Chemical Engineering Department, State University of New York at Buffalo, Buffalo, NY 14260, USA

Up to now, calcium carbide has been produced on an industrial scale exclusively by the electrothermal method. Very high-temperature operation should be used, and this results in high capital, and some serious environmental problems if open or half-covered furnaces are used. A chemical equilibrium calculation conducted in this laboratory shows that if we add a certain amount of argon into the precursors, the required temperature for chemical equilibrium of the system can be reduced to 1400–1500 °C. We have been guided to develop a d.c. plasma-heated fluidized bed for the preparation of calcium carbide. Preliminary experiments include cold fluidization, measurement of heat-transfer coefficient, production of calcium carbide and measurement of conversion rate. It was found that 84.3% conversion is reached in an argon atmosphere under atmospheric pressure and an operation temperature of 1400–1450 °C. X-ray diffraction analysis and SEM show that the generated calcium carbide is of good quality.

1. Introduction

Of all carbides, calcium carbide is still of the greatest industrial importance today. As a starting material it is now, as always, the basis of the acetylene welding-gas industry. If raw materials and energy are available and if petroleum is in short supply, calcium carbide is the starting material for the products of acetylene chemistry. In a number of countries this is as true today as ever before. The fertilizer (cyanamide) and the products derived from it, e.g. melamine, are still produced to a limited extent. In addition to these classical applications, calcium carbide is finding increasing use in the metallurgical field, where it is used for desulphurization of pig iron and steel, and in foundry technology, where it is mixed with other materials intended for metal treatment.

Increased acetylene usage for the production of organic chemicals, resins, and plastics increased the demand for calcium carbide. Annual production in the United States reached a maximum of 1027 000 metric tons in 1964, whereupon production declined substantially as acetylene from carbide was replaced by acetylene petrochemical sources, thermal cracking of hydrocarbons, and as a by-product in ethylene production. From 1975–1988 calcium carbide production ranged from 175 000–253 000 tons/year.

However, until now, calcium carbide has been produced on an industrial scale exclusively by electrothermal (resistance-type electric furnace and electric arc furnace) methods [1–7]. The electrothermal smelting methods operate with high CaO losses of as much as 22% of the charge. The calcium carbide yields amount to only 79%–84%. The market price of CaC_2 was about \$515/ton. Generally, calcium carbide is produced in electrical furnaces at a temperature around 2000 °C. Because of the high-temperature operation, the electrothermal smelting method induces some problems: (1) in order to keep the furnaces at high temperature, heat losses are very serious, and therefore the thermal efficiency is very low; (2) high-temperature operation requires high-quality materials for the construction of the facilities. Moreover, because the present production process is conducted in furnaces, the transportation processes of heat and mass between precursors are relatively slow, and so the kinetic process requires a relatively long time. All three factors result in high capital for production. Because of the rapidly growing oil-base ethylene derivatives, it is now necessary for us to make the price of CaC_2 cheaper.

During 1940–1960, the carbothermic process was used as a high technology route to make calcium carbide in Germany by BASF [8]. This process has recently again acquired economic interest, because the energy produced by the combustion of fuels with oxygen is not as expensive as electrical energy. Moreover, the CO gas abundantly produced as a by-product is a starting material for organic chemicals.

Recently, Japanese scientists made some significant improvement to the energy-saving type electric furnace to strengthen further the cost competitiveness of the calcium carbide produced [9].

A chemical equilibrium calculation conducted in this laboratory shows that if we add a certain amount of argon or hydrogen to the precursors, the required temperature for chemical equilibrium of the system

*Author to whom all correspondence should be addressed.

0022–2461

can be reduced to 1400–1500 °C. We have been guided to apply the fluidized-bed technology to the process, because by using this technology, the chemical reactions in the system can be pushed to be favourable for the formation of CaC_2 by using argon as the working gas and also the heat and mass transfer in the system can be speeded up, and in this case the required reaction temperature and reaction time can be reduced.

Three kinds of fluidized bed have been tried in our research: (1) a resistance-type fluidized bed; (2) a plasma-heated fluidized bed; (3) a flame-heated fluidized bed. Here we will describe the d.c. plasma-heated fluidized bed in detail.

During recent years, there has been some development in the aspect of a fluidized bed heated by plasma [10]. Its main applications include [11–14] plasma nitriding of titanium particles, plasma surface treatment of milled carbon fibre, and the hydrocracking process of heavy hydrocarbons. However, only r.f. plasma has been used as a power source. Because of the maturity and high efficiency (approximately 90%) of d.c. plasma, and also because of the flexibility of the adjustment of the operational parameters and the high purity of the plasma working gas, it seems that it is more valuable to develop a fluidized bed heated by d.c. plasma.

The aim of the present work was to develop a d.c. plasma-fluidized bed reactor for the preparation of calcium carbide. After presenting the chemical equilibrium calculation, details of the system are given. The initial experiment included cold fluidization, measurement of the heat-transfer coefficient, production of calcium carbide and measurement of the conversion rate. The generated calcium carbide was analysed by using X-ray diffraction and SEM. It was found that 84.3% conversion is reached under an operation temperature of 1400–1450 °C.

2. Chemical equilibrium calculation

Calcium carbide is a high-tonnage product of industry. It is known that it can be formed by the following reactions [15]

$$CaO + C \rightarrow Ca + CO \quad (1)$$

$$Ca + 2C \rightarrow CaC_2 \quad (2)$$

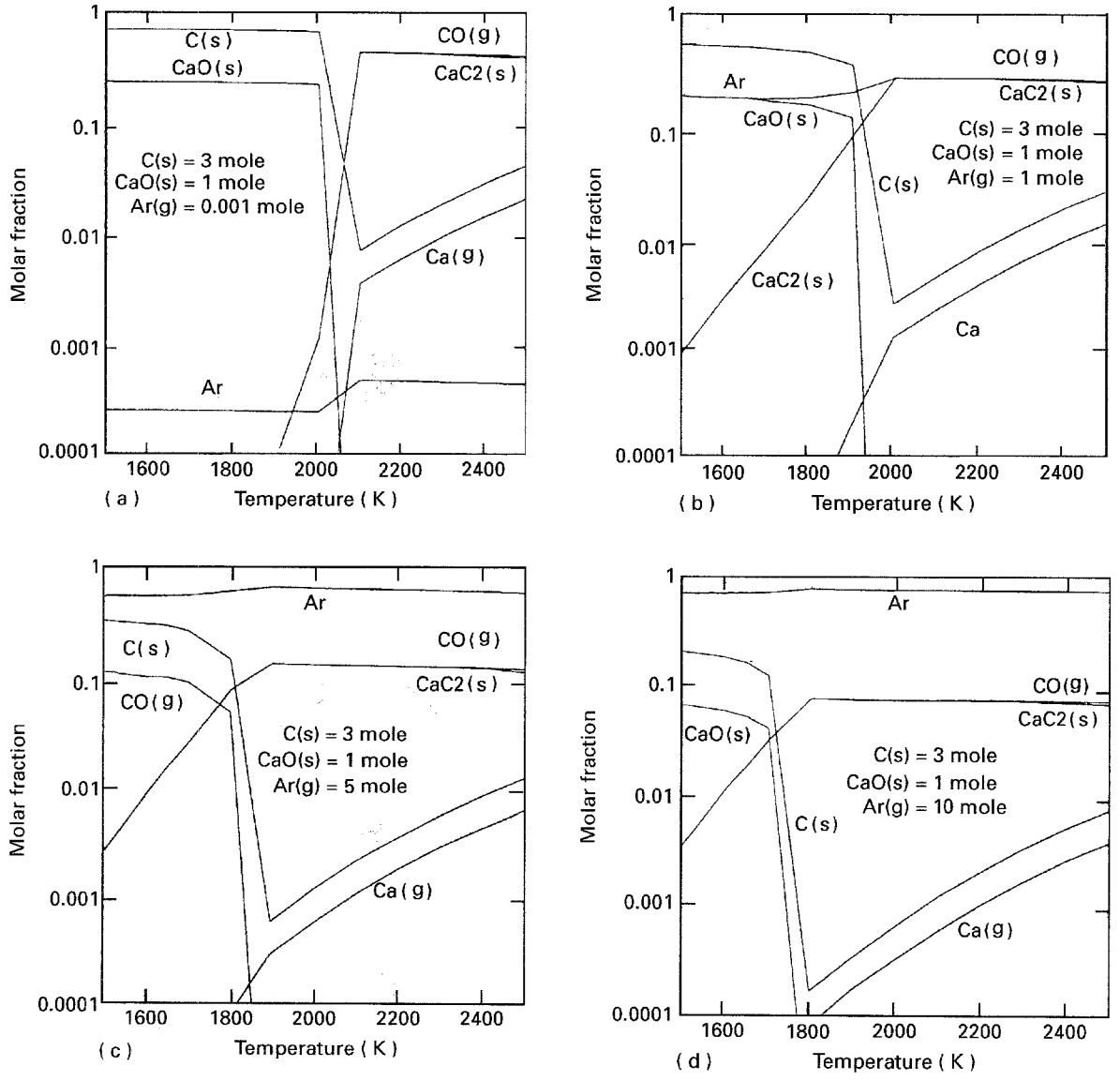

Figure 1 (a–d) Chemical equilibrium calculations for the system CaO + 3C + Ar.

where Reaction 1 occurs in the solid phase. Those are endothermic reactions, and the total reaction heat is 465 kJ mol^{-1}. Generally speaking, these reactions occur about 1800 °C. In order to determine the effect of some inert gas on the chemical reactions, a thermodynamic calculation was conducted using a NASA code [16] which was based on the minimization of Gibbs free energy. The specific heat, entropy and enthalpy of each species were taken from the JANAF thermodynamic tables [17]. The calculation is specific for the CaO + 3C + Ar system, 16 gas species and 5 condensed phases (C, CaO, CaC_2, $CaCO_3$, Ca) were considered. Fig. 1a–d show the formation of CaC_2 under an argon atmosphere at atmospheric pressure. The calculation obviously reveals that CaC_2 begins to form at 1700–1800 °C with a very small amount of argon. The temperature for the formation of CaC_2 decreases gradually with increase of the argon molar fraction; when the molar ratio of argon to CaO is 10, this temperature decreases to 1400–1500 °C. This result shows that with the dilution of the by-products such as CO, the chemical reaction will be more favourable to the formation of CaC_2.

3. Experimental procedure

The experimental system used in our operation is shown in Fig. 2. It includes three parts: (A) a plasma-heated fluidized bed reactor; (B) a d.c. plasma power supply; (C) a fluidization simulator.

3.1. Plasma-fluidized bed reactor

The design and fabrication of a d.c. plasma-fluidized bed reactor is a tedious job and should be handled very carefully. The plasma-heated fluidized bed used in this experiment is shown in Fig. 3 and can be divided into two parts.

3.1.1. Plasma torch

Several components were identified with the d.c. plasma torch: cathode, anode, water-cooling jacket, plasma gas and power input system. The cathode was fabricated using standard design with a 60° conical tip made up of thoriated tungsten (tungsten- and zirconium-alloyed tungsten were kept as stand-bys). The anode was made of copper, and a convergent throat shape with a nozzle of 6 mm diameter. The length of the anode can be changed very easily according to requirement (this may be called an arc plasma torch, where plasma stabilization takes place by eddy gases). The plasma gases were injected into the system tangentially and passed through the gap between the cathode and the anode created by a special swirling channel (a large swirling velocity is necessary for a stable plasma arc). These gases were simultaneously passed through four screens mounted in series in front of the anode to reduce the turbulence. The first three screens were of 250 mesh size and last 100 mesh size. The distance of the gap between the cathode and the anode was adjustable by a screwing arrangement, which is important to the operation condition of the

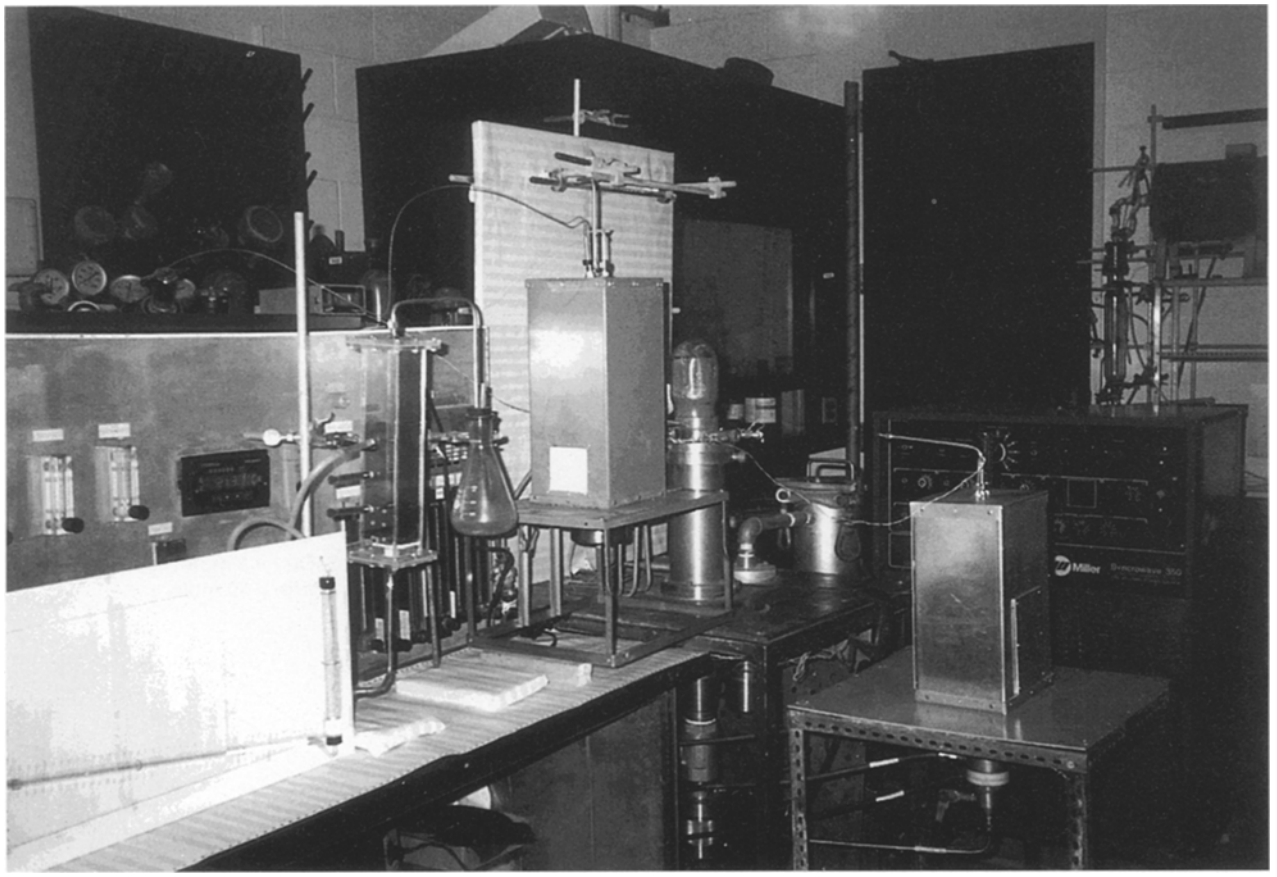

Figure 2 A photograph of the d.c. plasma-heated fluidized bed system for the production of CaC_2.

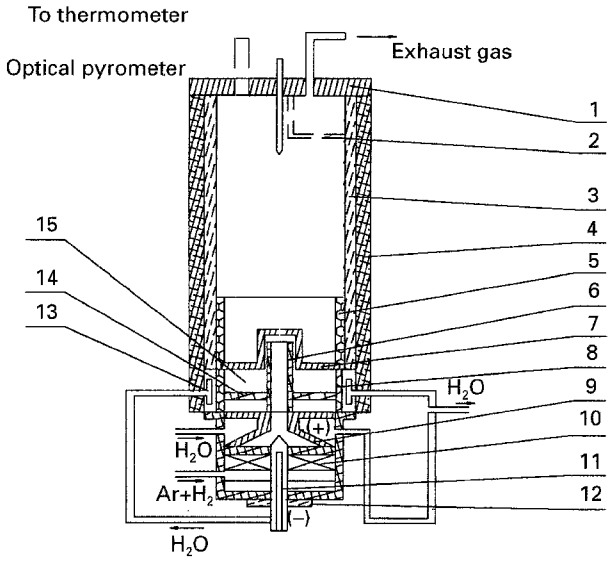

Figure 3 Experimental layout of the d.c. plasma-heated fluidized bed reactor. 1, Reactor cover; 2, powder filter; 3, refractory brick; 4, thermal insulation layer and metal wall; 5, protection graphite tube; 6, graphite tube; 7, distributor; 8, thermal insulation layer; 9, anode; 10, screens and passage of swirling gas; 11, cathode; 12, electrode adjustor; 13, waterjacket; 14, thermal insulation plate; 15, wind-box.

torch. An important cooling system was provided for both cathode and anode. The power supply was connected to cathode and anode by the cooling-water output lines; the anode was electrically grounded.

3.1.2. Plasma-heated fluidized bed reactor

Plasma-heated fluidized bed reactor is sited above the plasma torch. The plasma tail flame gas is transported into the windbox through a graphite tube, as shown in Fig. 3. In order to avoid the possible dropping of the powder into the bed through the holes on the top of the distributor, which can affect the electrical discharge and even induce damage of the electrodes, the plasma tail flame gas exits through the holes which are located on the side wall of the graphite tube. The cross-section of the bed is 50 mm × 50 mm. The height of the bed and freebroad is 300 mm. The reactor wall consists of a layer of refractory brick, a layer of thermal insulation material and an external metallic wall, as shown in Fig. 3. In order to protect the refractory brick (its temperature limit is about 1400 °C), a water-cooling system is used. Also a layer of insulation material is attached to the wall of the windbox to avoid loss of heat from the plasma tail flame gas. A layer of graphite is attached to the reactor wall in the fluidized bed section. The function of this layer is to protect the refractory brick wall from the high temperature of the fluidized bed. Because the thermal conductivity of graphite is relatively very large, it will enhance the temperature uniformity inside the bed. Underneath the fluidized bed is a distributor specially designed for the reactor. Details of the design will be specified later. The working gas exhausts from the exit located at the top of the freebroad. A powder filter made of a carbon fibre layer is mounted in front of the exit tube as a "flytrap" to avoid the possible flying out of the powder reactants.

Before each experiment, the powder is fed into the fluidized bed reactor. Then the top cover is closed and the exit hole and the powder filter are fixed. The top cover is opened 1–2 h after an experiment is finished in order to remove the product. During this time, a small argon flow rate is maintained to protect the product from moisture and to cool down the system.

3.2. D.c. plasma power supply

The maximum open circuit voltage of the power supply was 59.4 V, and the permissible maximum current 230 in the continuous operation. The power supply had an HF source with a frequency of 1 MHz and a voltage of 3000 V, which could be used to start the discharge of the d.c. torch. The power supply could maintain any constant current value in the permissible range, according to the adjustment (see [18] for details).

3.3. The fluidization simulator and the design of the distributor

The design of the distributor is of vital importance for the operation of the bed reactor. In order to simplify the structure of the fluidized bed and to save the working gas, no other gas except the plasma tail flame gas is used as working gas for the fluidization. Therefore, the distributor should be well-designed so that the required power of the fluidized bed and the amount of plasma gas for fluidization should be well matched through design. In the meantime, the temperature of the plasma tail gas is higher than 3000 °C in the graphite tube, and possible overheating of the reactor wall, and possible enlargement of the small holes on the distributor, must also be considered during design.

After repeated design and testing, the distributor shown in Fig. 4 is currently in use. The areas of the bottom cross-section and the top cross-section are 50 mm × 50 mm and 20 mm × 20 mm, respectively. The height of the distributor is 30 mm. There are 56 holes in a diameter of 0.8 mm on the bottom cross-section. On the top cross-section, there are 5 holes of the same diameter. The special shape of the distributor guarantees that the major part of the heat within the plasma tail flame gas can be transferred to the materials within the fluidized bed. In order to assist the design, the heat-transfer coefficient was measured systematically as shown in the next section. Because the plasma tail flame gas firstly passes the central projecting part of the distributor, this kind of passage avoids the direct contact of the high-temperature plasma tail flame gas with the reactor wall and overcomes the so-called "burn-through" problem on the reactor wall, which once occurred at the beginning of the experiment with other structures of the distributor.

Under the working temperature, it is very difficult to test and observe the fluidization in the reactor; therefore, a fluidization simulator was manufactured to test the fluidization in cold-working gas. The inside

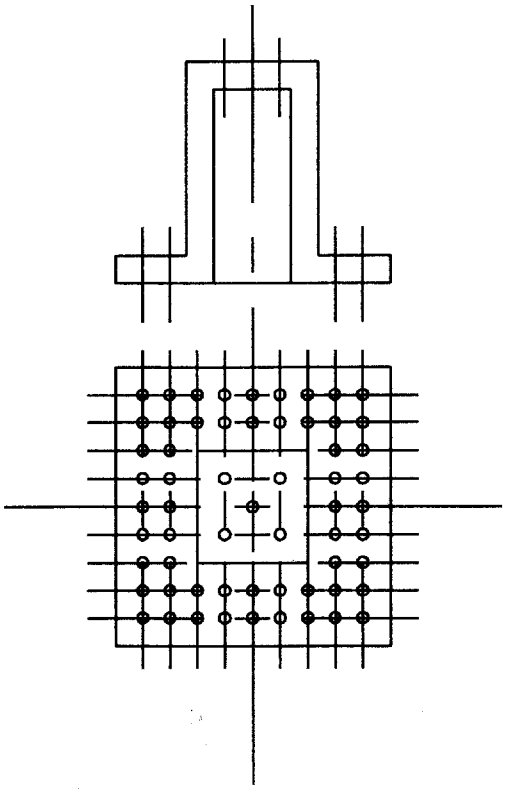

Figure 4 The distributor of the fluidized bed.

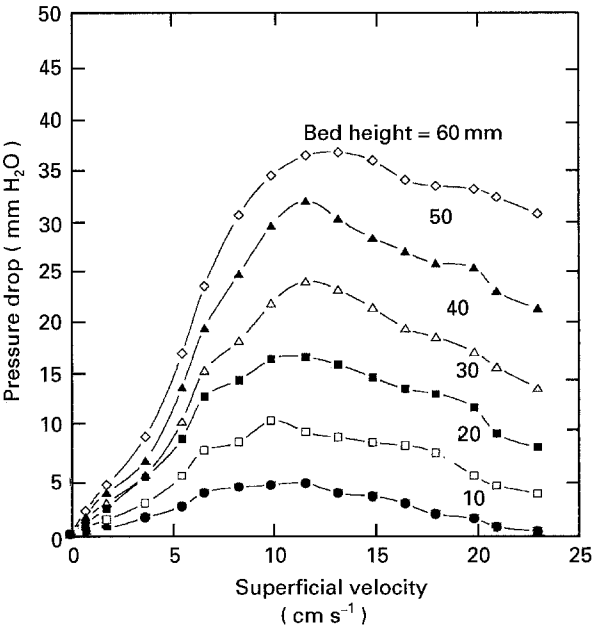

Figure 5 Pressure drop of the fluidized bed reactor with CaO and 3C particles. Measurements from the simulator. Size (mm): $0.355 < x_a < 1.0$. $\rho_p = 0.976\,g\,cm^{-3}$, in air.

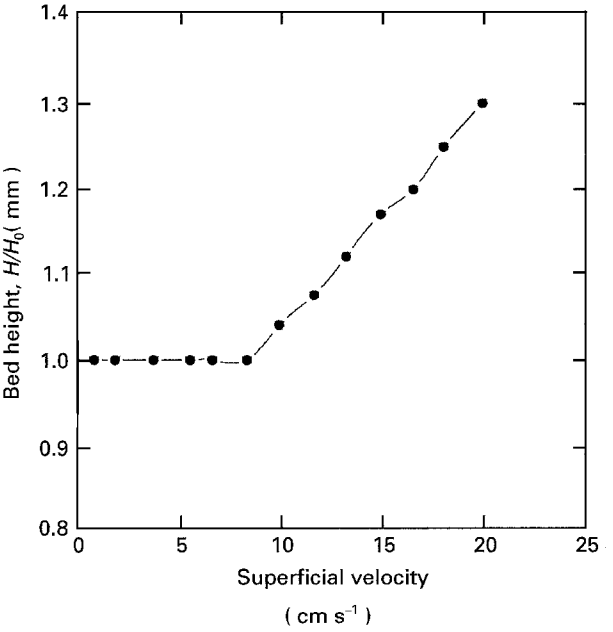

Figure 6 Bed expansion of the fluidized bed reactor. Size (mm): $0.355 < x_a < 1.0$. $\rho_p = 0.976\,g\,cm^{-3}$, in air. Powder: CaO + 3C. H = bed height, H_0 = initial bed height.

configuration and size of the fluidization simulator is the same as that in the fluidized bed reactor. The simulator is made of transparent reinforced plastic glass. Flow rate is measured by a set of rotameters. There are four holes along the windbox, bed and freebroad. Pressure drop along the four holes can be measured through an inclined monometer. The real structure can be seen in Fig. 2. A typical measurement is shown in Figs 5 and 6. From these measurements the minimum fluidization velocity was found to be $8\,cm\,s^{-1}$, i.e. the required gas flow rate is $0.7\,m^3\,h^{-1}$. When the bed reactor is heated to high temperature, the parameters obtained at low temperature for fluidization should be modified before use. For particles with different size and different physical properties there exist differences in their fluidization parameters between low temperature and high temperature. For instance [19], for the particles with diameters less than 2 mm, the fluidization velocity increases with the increase of temperature, but for those particles with diameters larger than 2 mm, the fluidization velocity decreases with increasing temperature. At high temperature, some particles exhibit viscosity, and experiment shows that the fluidization velocity is different for particles with different viscosity. However, in our experiment, we always keep the particle size less than 2 mm, and the superficial velocity twice the minimum fluidization velocity from the simulator, in order to guarantee the fluidization.

3.4. Measurement of heat-transfer coefficient

The heat-transfer coefficient is a very important parameter for the fluidized bed design and operation as mentioned in the previous section. Because the heat transfer between the plasma tail flame gas and the distributor is concentrated in the central projecting part of the distributor, the following relationship is used

$$Q = h(T_s - T_b)S \tag{3}$$

to give the heat-transfer coefficient. Fig. 7 shows the relationship of heat transfer coefficient, h, and superficial velocity, V, where T_s is the average surface temperature of the central projecting part of the distributor, and T_b is the average temperature of the fluidized bed. Q is the heat loss of the plasma tail flame gas after it passes through the graphite tube and the

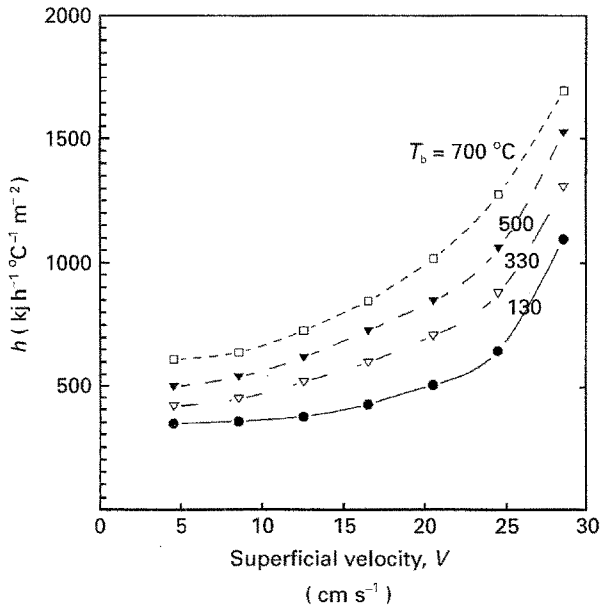

Figure 7 Measurement of the heat-transfer coefficient for the fluidized bed reactor in argon. Powder: CaO + 3C; size (mm): $0.71 < x < 1.0$. $Q = G_pC_p(T_i - T_e) = h(T_s - T_b)S$.

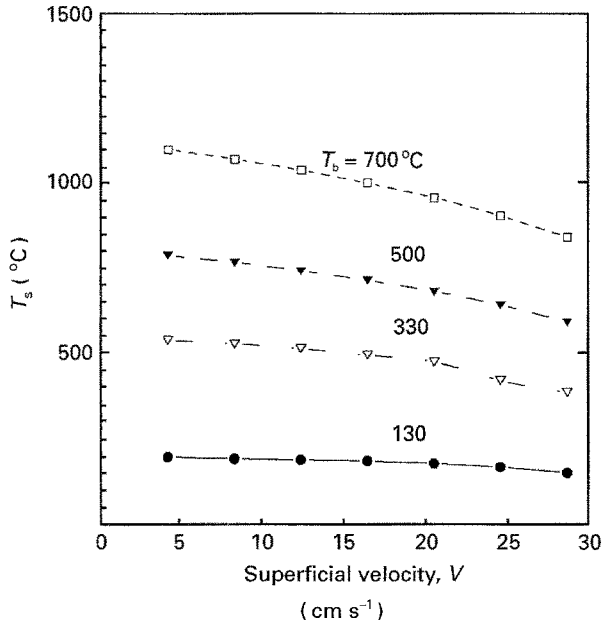

Figure 8 Measurement of the surface temperature on the distributor and the averaged bed temperature, in argon. Powder: CaO + 3C; size (mm): $0.71 < x < 1.0$.

central projecting part of the distributor, which can be calculated as the following

$$Q = G_pC_p(T_i - T_e) \quad (4)$$

where G_p is the flow rate from the torch (because there are five holes on the top of the central projecting part of the distributor, some modification was made for the calculation of the real value of G_p), T_i the temperature in the graphite tube at the position of the bottom section of the distributor, T_e the temperature of the plasma tail flame gas after it passes the central projecting part of the distributor, and S is the total surface of the central projecting part of the distributor. Measurement showed that the value of T_e is very near that of T_b. This result is what we expected when we made the design. Fig. 8 shows the relationship between the average temperature T_s and the superficial velocity at different bed temperatures. Most of the measurements were conducted by using thermocouples made of W/5%Re–W/26%Re, some of the measurements were conducted by using an infrared pyrometer. The model of the pyrometer used in the experiment is M77E, manufactured by Mikron Instrument Company Inc., which is a completely self-contained two-colour radiometer with the measurement range of 1100–2100 K and an accuracy of $\pm$ 0.75%.

4. The production of CaC_2 and the preliminary results of the experiment

In order to produce CaC_2 with high quality and high quantity in a fluidized bed, except for the well-designed fluidized bed, other problems must be solved. The raw material must satisfy the technical requirement of the working conditions in the plasma-fluidized bed. As we know, the chemical reactions proceed within the solid particles, the fluidized bed affords a very high-temperature environment and the heat required for the high endothermic reaction. The working gas within the bed also plays an important role in removing gaseous by-products such as CO, CO_2, and then pushing the chemical reaction forward to reach the equilibrium at the bed temperature under conditions without those gas by-products. Based on the above analysis, the requirements include (1) the shape and the size of the particles should be good for their fluidization, (2) within every particle, the stoichiometric ratio of reactants should be correct, (3) the connection between carbon and calcium oxide particles should be strong enough to withstand high temperatures, and the mechanical forces induced during the operation which include friction force, collision force between particles, particles and the wall of the reactor, particles and the distributor. There are several ways to manufacture such particles. Herold *et al.* [20] used CaO small particles as the core to coat a carbon film in order to produce the required particles for their operation in a flame reactor. Another way which was developed in our laboratory was to mix carbon and CaO powders according to the stoichiometric ratio of CaO + 3C and form pellets under high pressure ($\sim 150\,000$ N cm^{-2}) with some bonding, then those pellets are broken into small particles of the required size.

Recently, two kinds of material have become available in the laboratory for the experiments. The first is from South Africa. The diameter of the particles is about 3–5 mm. Every particle is a combination of CaO and carbon. They were stuck together by some bonding. Because those particles are very loose, during the experiment, much small powder drops from them. The other kind of material is also from South Africa, and this is big blocks of lime (95% CaO) and big blocks of anthracite (77% C).

The following tests have been conducted on those two materials.

1. Direct experiment with the particles of diameter 3–5 mm. Because the particle size is very large, the

cold fluidization requires a large amount of argon. In order to save gas, we use a small flow rate. The fluidization cannot be achieved during the cold-state test. However, during the high-temperature test, it seems that the bed is fluidized because small hot particles are blown out from the exit of the reactor. The test temperature is 1400–1450 °C. Because this kind of particle is very loose and the materials within them are non-uniform, the resulting conversion rate is different for different particles. Some reach very high values (up to 80%), some are very low, some even have zero conversion rate.

2. The above particles are broken into particles about 1 mm in diameter. It is very easy to fluidize this kind of particles, both at low and high temperature. Because the materials contained in the particles are not in the correct stoichiometric ratio for the production of CaC_2 after breaking, after the operation the conversion rate is much more non-uniform and much lower that in the above case. We frequently find pure white and black powders in the product. The operation temperature is 1400–1450 °C.

3. The big blocks of lime and anthracite are broken into small particles, about 0.7 mm diameter and are mixed together without bonding. The resulting conversion rate for this kind of raw material is very low, even though some smell of C_2H_2 from the product can be detected.

4. The big blocks of lime and anthracite are broken into small particles, of less than 0.2 mm diameter. These are mixed together with the correct stoichiometric ratio of CaC_2. Then the mixture is pressed into pellets. Part of the pellets are broken into small particles of less than 2 mm diameter and then fed into the fluidized bed. The reaction is kept under 1400–1450 °C. Because the small particles can easily move around the big pellets during the operation, this enhances the transport process between the solid material and working gas, and eventually very satisfactory results are obtained. With this kind of material the operation should be very carefully performed, as most of the pellets and particles are very easily broken.

The products produced in case 4 were analysed using X-ray diffraction and SEM. Fig. 9 shows the X-diffraction pattern which verifies that the produced CaC_2 is of very good quality with a very small amount of impurity. The peaks at $2\theta = 26.8°$, 32.8°, 43.4°, 46.8° and 55.3° are standard values for CaC_2. Fig. 10 shows that the produced CaC_2 is formed of very uniform and small crystal grains. The cracking in the picture is induced by the rapid moisturizing of some parts of the product. Table I gives the conversion rate, which was directly measured from the product assuming that there was no impurity within the product.

5. Discussion and conclusion

Guided by a chemical equilibrium calculation, we have successfully developed a d.c. plasma-heated fluidized bed reactor for the preparation of calcium carbide. Preliminary experiments, including cold fluidization, measurement of the heat-transfer coefficient, production of calcium carbide and measurement of the conversion rate, were conducted. The major

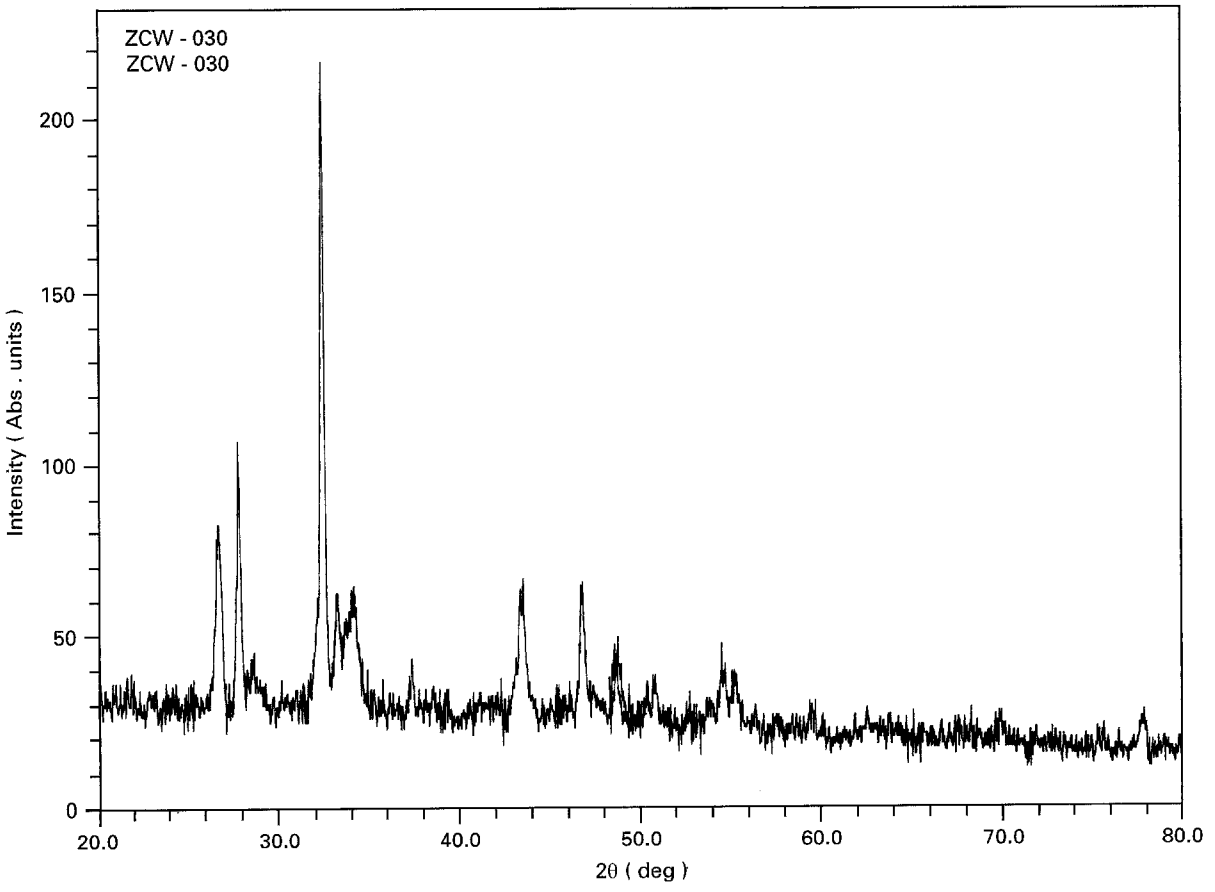

Figure 9 X-ray diffraction of the produced CaC_2.

Figure 10 Scanning electron micrograph of the produced CaC_2.

TABLE I Preliminary results for the production of CaC_2 in a plasma-fluidized bed reactor. The results give a conversion rate of 84.3%. This is measured directly from the product assuming that there is no impurity within the product. In fact, there is some impurity inside the product, which was not evaporated during the operation. If this point is considered in the analysis, the conversion rate may be higher

Raw materials	Operating temperature (°C)	Reaction time (min)	Conversion rate	X-ray
Lime (95% CaO) Anthracite (77%C)	1400–1450	40	84.3	Good

advantage of this method is that the temperature and reaction time required for the production of calcium carbide are much lower than those used in the furnaces in operation today.

Another advantage of the present method is that the production process is very clean and there is very low material loss during the operation. The generated calcium carbide was analysed by X-ray diffraction and SEM. A conversion rate of 84.3% was reached under the reaction temperatures of 1400–1450 °C and a reaction time of 40 min.

A high conversion rate can be achieved only in a suitable raw material. A mixture of carbon particles and CaO particles without bonding gives a very low conversion rate. A high conversion rate can be reached using the preparation method (case 4) developed by the authors.

In order to scale up the process, it seems that many more tests should be performed, for instance, the dependence of the conversion rate on the reaction time, the effect of particle size of carbon and CaO powders which are used to make the raw material and the raw material particle size on the conversion rate, etc. The results of these tests will be published elsewhere.

References

1. HELMUT VON ZEPPELIN, MOLHIN, HEINZ KALHAMMER, WALDSHUT and KLAUS HOHMANN, Swiss Pat. 437 228 (1967).
2. M. FRANKL, US Pat. 2131 102 (1938).
3. BOIS EASTMAN, US Pat. 3017 259 (1920).
4. BRUCE H. SAGE, US Pat. 3044 858 (1962).
5. N. V. STAMICARBON, Br. Pat. 863 191 (1959).
6. *Idem*, Br. Pat. 737 857 (1955).
7. KES VAN LOON, US Pat. 2814 478 (1957).
8. "Ullmann's Encyclopedia of Industrial Chemistry", Vol. 4 (VCH, Deerfield Beach, USA, 1985).
9. S. KIRITANI and T. NISHIMAKI, *Chem. Economy Eng. Rev.* **16**(5) (1984) 27.
10. S. MOROOKA, T. OKUBO and K. KUSAKABE, *Powd. Technol.* **63** (1990) 105.
11. T. OKUBO, H. KAWAMURA, K. KUSAKABE and S. MOROOKA, *J. Am. Ceram. Soc.* **73** (1991) 1150.
12. H. KAWAMURA, *J. Mater. Sci. Lett.* **9** (1990) 1033.
13. M. NIKRAVECH, L. OUTIFA and J. E. AMOUROUX, "Plasma-fluidized bed hydrocracking process of heavy hydrocarbons", ISPC-9 Japan (1989).
14. PH. ARNOULD, S. CAVADIAS, J. AMOUROUX and P. H. ARNOULD, "The interaction of a fluidized bed with a thermal plasma. Application to the limestone decomposition", 7th International Symposium of Plasma Chemistry, Eindhoven, July 1985.
15. A. N. EFIMOV, M. I. ZHIKHAREV and YU. P. ZHIRNOV, *At. Energ.* **39** (1975) 416.
16. S. GORDEN and B. J. McBRIDE, NASA SP-237 (1976).
17. D. R. STULL and H. PROPHET (eds), "JANAF Thermochemical Tables", 2nd Edn (1971).
18. C. W. ZHU, G. Y. ZHAO and V. HLAVACEK, *J. Mater. Sci.* **27** (1992) 2211.
19. R. R. PATTIPATI and C. Y. WEN, *Ind. Eng. Chem. Process Des. Dev.* **20** (1981) 705.
20. HEROLD Y. ATWELL and N. Y. FISHKILL, US. Pat. 3017 244 (1962).
21. H. S. MICKLEY, *A.I.Ch.E J.* September (1955).
22. J. S. M. BOTTERILL, *A.I.Ch.E Symp. Ser.* 208 **77** (1881) 330.

Received 6 September 1993
and accepted 13 October 1994